

Diatomic Hönl–London factor computer program

James O. Hornkohl, Christian G. Parigger, and László Nemes

A new method is presented for computation of diatomic rotational line strengths, or Hönl–London factors. The traditional approach includes separately calculating line positions and Hönl–London factors and assigning parity labels. The present approach shows that one merely computes the line strength for all possible term differences and discards those differences for which the strength vanishes. Numerical diagonalization of the upper and lower Hamiltonians is used, which directly obtains the line positions, Hönl–London factors, total parities, and e/f parities for both heteronuclear and homonuclear diatomic molecules. The FORTRAN computer program discussed is also applicable for calculating n -photon diatomic spectra. © 2005 Optical Society of America

OCIS codes: 300.6390, 140.3440, 350.5400.

1. Introduction

The rotational line-strength factor, also called the Hönl–London¹ factor (HLF), is one of the more important terms in the equations for diatomic line intensities. The relative intensities of diatomic spectral lines are primarily controlled by the state population density and the HLF. Computed diatomic spectra are of inherent value because comparison of a synthetic spectrum with a recorded spectrum allows one to compare experiment with theory. Figure 1 shows such a comparison with experimental results that were recorded by Roux *et al.*² However, synthetic diatomic spectra are most widely used in applied spectroscopy as diagnostic tools. This paper particularly addresses spectroscopy of diatomic molecules for diagnostics applications. Although the summary on spectroscopy will be familiar to all spectroscopists, it will be particularly useful for researchers in areas of combustion, aerodynamics, materials processing, atmospheric measurements, astrophysics, and the many other areas where diatomic spectroscopy has a long and expanding record as a diagnostic measurement tool. The discussion below uses established, for-

mal methods to utilize the theory of diatomic spectroscopy in practical applications.

The process of free spontaneous emission is selected for introducing the terminology “line strength.” The radiation emitted isotropically per unit time from a unit volume of excited gas molecules that radiatively decay from upper state u to lower state l is described by

$$I_{ul} = h\nu_{ul}A_{ul}N_u, \quad (1)$$

where h is Planck’s constant, $\nu_{ul} = c/\lambda_{ul}$ is the frequency for the spectral line of wavelength λ_{ul} , A_{ul} is the Einstein A coefficient or transition probability, and N_u is the number density of the excited state u . The quantity I_{ul} is the power density of the emitted radiation,

$$I_{ul} = \frac{dE}{dt dV} = \frac{dP}{dV}. \quad (2)$$

The dimensional interpretation of Eq. (1) is

$$\begin{aligned} I_{ul} \left(\frac{\text{joules}}{\text{second volume}} \right) &= h\nu_{ul} \left(\frac{\text{joules}}{\text{photon}} \right) \\ &\times A_{ul} \left(\frac{\text{photons}}{\text{molecule second}} \right) \\ &\times N_u \left(\frac{\text{molecules}}{\text{volume}} \right). \end{aligned} \quad (3)$$

In thermal equilibrium the population density of excited states is given by

J. O. Hornkohl (jhornkoh@utsci.edu) and C. G. Parigger (cparigge@utsci.edu) are with The University of Tennessee Space Institute, 411 B. H. Goethert Parkway, Tullahoma, Tennessee 37388. L. Nemes (nemesl@cric.chemres.hu) is with the Laboratory for Laser Spectroscopy, Chemical Research Center, Hungarian Academy of Sciences, Pusztaszeri ut 59-67, H-1025 Budapest, Hungary.

Received 1 September 2004; revised manuscript received 10 March 2005; accepted 25 March 2005.

0003-6935/05/183686-10\$15.00/0

© 2005 Optical Society of America

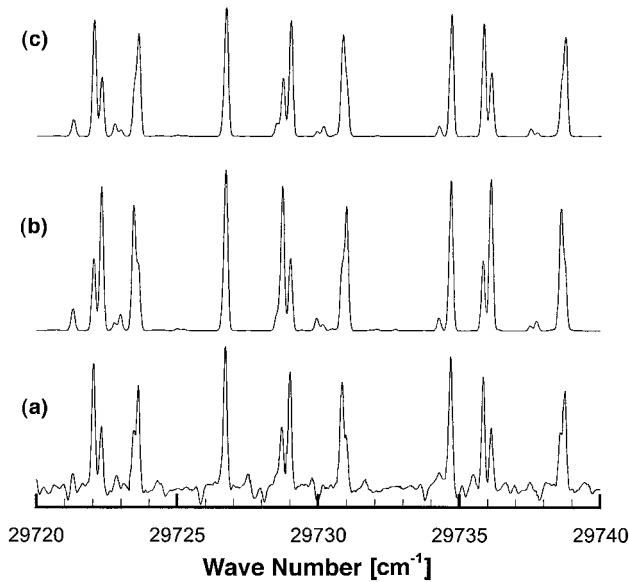


Fig. 1. Example of using computed diatomic spectra to reveal the significance of parity assignments. (a) Section of a Fourier transform spectrum of the $C^3\Pi_u \leftrightarrow B^3\Pi_g$ band of a system of N_2 recorded by Roux *et al.*² Their high-resolution spectrum shows a 2:1 alternation of intensities in the resolved Λ doublets. (b) Computed spectrum in which the alternation of intensities in the Λ doublets is the reverse of that seen in the experimental spectrum, thus showing the significance of a reversal of parity assignment. (c) Spectrum computed with the correct parity assignment.

$$N_u = N_0 \frac{g_u \exp(-E_u/k_B T)}{Q}, \quad (4)$$

where N_0 is the total population density of molecules, g_u is the statistical weight of the state u , E_u is the energy eigenvalue for state u , k_B is Boltzmann's constant, T is the absolute temperature, and Q is the partition function or state sum,

$$Q = \sum_i g_i \exp\left(-\frac{E_i}{k_B T}\right). \quad (5)$$

Combining Eqs. (1) and (4) gives

$$I_{ul} = h\nu_{ul} A_{ul} N_0 \frac{g_u \exp(-E_u/k_B T)}{Q}. \quad (6)$$

The total population density N_0 , the partition function Q , and the absolute spectral sensitivity of the apparatus are needed to compute a synthetic spectrum suitable for comparison with measurements. Much more common are comparisons between predicted and measured relative spectral intensities of individual band systems for which the total population density and partition function are not required.

The spontaneous emission Einstein A coefficient is only one of several quantities related to the intensity of spectral lines. The Einstein absorption B_{lu} and stimulated emission B_{ul} coefficients and the absorption oscillator strength f_{lu} are widely used, but each of

these can be defined in terms of a more fundamental and symmetrical quantity, i.e., the line strength S_{ul} .^{3–5} For example, the spontaneous emission Einstein A coefficient is related to the line strength as follows:

$$A_{ul} = \frac{64\pi^4 \nu_{ul}^3}{3hc^3 g_u} S_{ul}. \quad (7)$$

The occurrence of the statistical weight g_u in Eq. (6) appears as a complicating factor. Written in terms of the line strength, the equation for free spontaneous emission from thermally excited states reads as

$$I_{ul} = \frac{64\pi^4 N_0}{3c^3 Q} \nu_{ul}^4 S_{ul} \exp\left(-\frac{E_u}{k_B T}\right), \quad (8)$$

in which the statistical weight does not explicitly occur. The statistical weights of diatomic states is a topic of some complexity that can often be avoided if the equations are written in terms of the line strength instead of Einstein coefficients or oscillator strengths.

A. Definition of the Line Strength

The defining equation for the line strength is^{6–9}

$$S_{ul} = \sum_u \sum_l |\langle u | T_k^{(q)} | l \rangle|^2, \quad (9)$$

in which the summations over u and l are carried over all states that produce the same observation (spectral line), and $T_k^{(q)}$ is the k th component of the irreducible tensor of order q responsible for the $u \leftrightarrow l$ transition. In the absence of applied fields, the summations are over the magnetic quantum numbers. For electric dipole transitions, the operator responsible for the transitions is the dipole operator, \mathbf{er} , and the equation for the line strength becomes

$$S(n'J', n''J'') = e^2 \sum_{M'} \sum_{M''} |\langle n'J'M' | x\hat{\mathbf{i}} + y\hat{\mathbf{j}} + z\hat{\mathbf{k}} | n''J''M'' \rangle|^2, \quad (10)$$

where e is the electronic charge and $\hat{\mathbf{i}}, \hat{\mathbf{j}}$, and $\hat{\mathbf{k}}$ are the unit vectors for the coordinate axes. In writing this equation we have replaced the simple $u \leftrightarrow l$ notation in favor of the more explicit spectroscopic notation in which J is the total angular momentum quantum number, M is the quantum number for the z component of the total angular momentum, n is a symbol for all other mostly electronic quantum numbers, and upper and lower states are denoted with single and double primes.

B. Rotational Line-Strength Factor

For a diatomic molecule the total line strength can often be satisfactorily approximated as the product of an electronic–vibrational strength $S(n'v', n''v'')$, which is expressed in units of line strength (i.e.,

coul² m² for electric dipole transitions), and of the unitless rotational line-strength factor or HLF $S(J', J'')$:

$$S(n'v'J', n''v''J'') = S(n'v', n''v'')S(J', J''). \quad (11)$$

The HLFs are often quite specific to the spectrum of interest. Numerous equations for HLFs can be found in the literature, some of which contain only angular momentum quantum numbers. For example, the HLFs for Hund's case $a \leftrightarrow$ case b transitions are given by

$$S_{aa}(J', J'') = (2J'' + 1) \langle J'' \Omega'' q, \Omega' - \Omega'' | J' \Omega' \rangle^2, \quad (12)$$

in which Ω is the quantum number for the component of the total angular momentum along the internuclear axis, q is the order for the transition, and $\langle J'' \Omega'' q, \Omega' - \Omega'' | J' \Omega' \rangle$ is the Clebsch–Gordan coefficient. Case $a \leftrightarrow$ case b HLFs are given by

$$S_{bb}(J', J'') = (2J' + 1)(2J'' + 1)(2N'' + 1) \times \langle N'' \Lambda'' q, \Lambda' - \Lambda'' | N' \Lambda' \rangle^2 \left\{ \begin{matrix} S & N'' & J'' \\ & k & J' & N' \end{matrix} \right\}^2 \times \delta(S', S''), \quad (13)$$

in which N is the quantum number for the total angular momentum exclusive of spin, Λ is the quantum number for the internuclear component of \mathbf{N} , and S is the quantum number for the total electronic spin. The symbol that consists of the curly braces and two included rows of quantum numbers is the Wigner 6- j symbol. The Clebsch–Gordan coefficients and Wigner 6- j symbols are important parts of the analytical description of the modern theory of angular momentum. Despite their apparent notational complexity, each is simply a mathematical function to be computed in a readily available subroutine.

The order q of the irreducible tensor $\mathbf{T}^{(q)}$ in Eqs. (9), (12), and (13), is, of course, an integer number for rotations. The HLFs reflect fundamental symmetries, and the order (or integer value) of the tensor operator specifies the type of transition. In other words, the HLFs contain the angular momentum part of the line strength.

Although Eqs. (12) and (13) serve as examples of the application of angular momentum theory, the case $a \leftrightarrow a$ and $b \leftrightarrow b$ HLFs have little practical implications. More typically, the HLF is controlled by the angular momentum quantum numbers as in Eqs. (12) and (13) and additionally by some spectroscopic constants such as B_v and A_v .

Numerous tables and equations for HLFs are available. Rubin,¹⁰ Kovacs,¹¹ and Hougen¹² discuss the calculation of HLFs. Schadee^{13–15} and Tatum¹⁶ discuss their use and give additional tables. Whiting *et al.*^{17,18} introduced numerical diagonalization of the Hamiltonian as a very significant improvement over analytical approximation for calculation of HLFs.

The algorithm described below is an extension of Whiting's work.

As with the term value equations, when one uses the HLF equations one must collect the relevant equations and the values for the constants in these equations and evaluate the equations over the desired range of quantum numbers. The final step is to collate the HLFs with the separately computed line positions. This tedious process may be complicated by the absence of a unique index for each of the upper and lower energy states or each spectral line.

2. Traditional Methods for Computing Diatomic Spectra

A synthetic spectrum is a graphical representation of intensity versus wavelength or wave number that is divided into wavelength bins. The contribution of intensity from each spectral line, from each of the radiating species, and to each wavelength bin is computed. The traditional methods of applied spectroscopy make this process rather involved.

Given at least one radiating species, one's first task in beginning the computation of a spectrum is the selection of the wavelength range and the number of bins into which this range will be broken. Both are normally dictated by specifications of spectroscopic equipment. The next step is computation of the line positions, i.e., wavelengths or wave numbers.

A. Term Value Equations

The term value (the energy divided by the product of Planck's constant h and the speed of light c) is the typical quantity used by spectroscopists. The vacuum wave number $\tilde{\nu}_{ul}$ is the difference between the upper and the lower terms

$$\tilde{\nu} = T_u - T_l, \quad (14)$$

and the vacuum wavelength λ_{ul} is the reciprocal of the wave number. Term values are traditionally computed from semiempirical term value equations such as

$$F_J = B_v J(J + 1) - D_v J^2(J + 1)^2 + H_v J^3(J + 1)^3 + \dots \quad (15)$$

for the rotational terms F_J and

$$G_v = \omega_e(v + 1/2) - \omega_e x_e(v + 1/2)^2 + \omega_e y_e(v + 1/2)^3 + \dots \quad (16)$$

for the vibrational terms. One obtains the spectroscopic constants ($B_v, D_v, \omega_e, \omega_e x_e$, etc.) from a reference source or journal article and computes the terms for a range of rotational and vibrational quantum numbers, J and v . The rotational and vibrational term value equations are combined in the Dunham expression

$$T_{vJ} = \sum_{i=0,1,\dots} \sum_{j=0,1,\dots} Y_{ij}(v + 1/2)^i [J(J + 1)]^j, \quad (17)$$

Table 1. Hund's Case *a* Hamiltonian Matrix Elements that Do Not Mix Electronic States^a

Hamiltonian Matrix Element	Value of Hamiltonian Matrix Element
$\langle n v S \Omega \Lambda \Sigma B_v \mathbf{R}^2 n v S \Omega \Lambda \Sigma \rangle$	$B_v[J(J+1) - \Omega^2 + S(S+1) - \Sigma^2]$
$\langle n v S \Omega \Lambda \Sigma B_v \mathbf{J} \cdot \mathbf{S} n v S \Omega \pm 1, \Lambda, \Sigma \pm 1 \rangle$	$B_v[J(J+1) - \Omega(\Omega \pm 1)][S(S+1) - \Sigma(\Sigma \pm 1)]^{1/2}$
$\langle n v S \Omega \Lambda \Sigma A_v \mathbf{L} \cdot \mathbf{S} n v S \Omega \Lambda \Sigma \rangle$	$A_v \Lambda \Sigma$
$\langle n v S \Omega \Lambda \Sigma \epsilon_v [3S_z^2 - \mathbf{S}^2] n v S \Omega \Lambda \Sigma \rangle$	$\epsilon_v [3\Sigma^2 - S(S+1)]$
$\langle n v S \Omega \Lambda \Sigma \gamma_v \mathbf{N} \cdot \mathbf{S} n v S \Omega \Lambda \Sigma \rangle$	$\gamma_v [\Sigma \Omega - S(S+1)]$
$\langle n v S \Omega \Lambda \Sigma \gamma_v \mathbf{N} \cdot \mathbf{S} n v S \Omega \pm 1, \Lambda, \Sigma \pm 1 \rangle$	$-\frac{1}{2} \gamma_v [J(J+1) - \Omega(\Omega \pm 1)][S(S+1) - \Sigma(\Sigma \pm 1)]^{1/2}$

^aEven for a single electronic state, the case *a* matrix elements do not compose a diagonal Hamiltonian matrix, indicating that Hund's case *a* is not desirable in a physical description. However, highly accurate diatomic solutions can be found by writing the eigenfunction as a sum of case *a* basis functions. This sum must always include at least two electronic states (e.g., $|^2\Sigma\rangle + |^2\Pi\rangle$) to ensure that the eigenfunction is indeed an angular momentum eigenfunction.

where $Y_{10} = \omega_e$, $Y_{20} = -\omega_e x_e$, $Y_{01} = B_e$, $Y_{11} = -\alpha_e$, $Y_{02} = -D_e$, and so forth. However, whereas the vibrational term value equation (16) is rather generic, the rotational term value equation (15) must often be replaced by a more complicated equation involving additional quantum numbers, such as Λ , Ω , S , Σ , and N , or by numerical diagonalization of a Hamiltonian matrix.

Even experienced spectroscopists often need to expend considerable effort to use the equations above. Moreover, term value equations are not applicable for high J and v and are often very spectrum specific. When using term value equations, one normally writes a new computer program whenever a new type of diatomic spectrum is studied, even in the same species. Another issue associated with term value equations is that it will require collation of the computed line positions with the separately computed line strengths.

B. Selection Rules

Subsequent to computation of the upper and lower term values, one must apply selection rules to determine which of the term value differences actually represent spectral lines. Construction of an algorithm for application of selection rules to term differences is difficult. There are angular momentum selection rules, parity selection rules, and (for homonuclear diatomics) exchange symmetry selection rules. Converting textbook rules into a general purpose algorithm is particular difficult for the lowest values of J' and J'' . When the terms and HLFs are computed separately, there is simply no general index with which one can easily collate the term value differences with the HLFs. The algorithm presented here alleviates the problem of inclusion of selection rules.

3. Program Algorithm

The algorithm for the program is as follows:

- Select a value for the upper total angular momentum quantum number J' .
- Select values for the lower total angular momentum quantum number J'' over the range

$$J'' = J' - q, J' - q + 1, \dots, J' + q, \quad (18)$$

where q is the order of the transition, Eq. (9); $q = 1$ for dipole transitions, $q = 2$ for two-photon or Raman transitions, etc.

- For each $J'-J''$ pair, compute the Hund's case *a* representation of the upper and lower Hamiltonians.
- Numerically diagonalize the upper and lower Hamiltonian matrices.
- Evaluate the HLFs for all term value differences. All transitions for which $S(J', J'')$ is nonvanishing are allowed. All transitions for which $S(J', J'') = 0$ are forbidden. This selection rule rigorously implements all selection rules.
- The parity eigenvalues are found by computing the Hund's case *a* matrix representation of the parity operator for the upper and lower states and then diagonalizing each parity matrix by applying the same orthogonal matrix that diagonalized the corresponding Hamiltonian matrix.
- The e/f parity designation is computed, as is the line designation (e.g., P_{12}), based on the values of J' and J'' . The ill-defined quantum number N (which would be the quantum number for the total electronic orbital angular momentum if this quantity were a constant of the motion) is estimated.

A. Hund's Case *a* Matrix Elements of the Hamiltonian

The central part of the algorithm described above is computation of approximate matrix representations of the upper and lower diatomic Hamiltonians for specified J' and J'' . The Hund's case *a* basis was chosen because it is well known and simple.¹⁹ Case *a* basis functions are given by

$$\langle \mathbf{r}_1 \mathbf{r}_2 \dots \mathbf{r}_N \mathbf{r} | n v J M \Omega \Lambda S \Sigma \rangle = \left(\frac{2J+1}{8\pi^2} \right)^{1/2} \langle \mathbf{R}'_e r | n v \rangle | S \Sigma \rangle D_{M \Omega}^{J*}(\alpha \beta \gamma), \quad (19)$$

where $\mathbf{r}_1 \mathbf{r}_2 \dots \mathbf{r}_N$ are the laboratory coordinate vectors for the N electrons, \mathbf{r} is the internuclear vector, and \mathbf{R}'_e denotes $3N - 1$ molecule fixed electronic coordinates (γ is the remaining electronic coordinate.)

Table 1 gives the case *a* matrix elements of the

Table 2. Hund's Case *a* Hamiltonian Matrix Elements that Mix Electronic States^a

Hamiltonian Matrix Element	Value of Hamiltonian Matrix Element
$\langle n v \Omega S \Lambda \Sigma B(r) \mathbf{J} \cdot \mathbf{L} n' v' \Omega \pm 1, \Lambda \pm 1, \Sigma \rangle$	$= \langle n v B(r) (L_+ + L_-) n' v' \rangle [J(J+1) - \Omega(\Omega \pm 1)]^{1/2}$ $= \langle BL \rangle_{nv, n'v} [J(J+1) - \Omega(\Omega \pm 1)]^{1/2}$
$\langle n v \Omega S \Lambda \Sigma B(r) \mathbf{L} \cdot \mathbf{S} n' v' \Omega \Lambda \pm 1, \Sigma \mp 1 \rangle$	$= \langle n v B(r) (L_+ + L_-) n' v' \rangle [S(S+1) - \Sigma(\Sigma \mp 1)]^{1/2}$ $= \langle BL \rangle_{nv, n'v} [S(S+1) - \Sigma(\Sigma \mp 1)]^{1/2}$
$\langle n v \Omega S \Lambda \Sigma A(r) \mathbf{L} \cdot \mathbf{S} n' v' \Omega \Lambda \mp 1, \Sigma \pm 1 \rangle$	$= \langle n v A(r) (L_+ + L_-) / 2 n' v' \rangle [S(S+1) - \Sigma(\Sigma \mp 1)]^{1/2}$ $= \langle AL \rangle_{nv, n'v} [S(S+1) - \Sigma(\Sigma \mp 1)]^{1/2} / 2$
$\langle n v \Omega S \Sigma A(r) \mathbf{L} \cdot \mathbf{S} n' v' \Omega S' \Lambda' \Sigma' \rangle$	$= \langle A \rangle_{nv\Lambda\Sigma, n'v'\Lambda'\Sigma'} (-)^{\Lambda'-\Lambda} \langle S' \Sigma', 1, \Lambda' - \Lambda S \Sigma \rangle$
$\langle n v \Omega S \Lambda \Sigma \alpha(r) \mathbf{S}^2 n v \Omega S, \Lambda \pm 2 \Sigma \mp 2 \rangle$	$= \alpha_v [S(S+1) - \Sigma(\Sigma \pm 1)]^{1/2} [S(S+1) - (\Sigma \pm 1)(\Sigma \pm 1)]^{1/2} / 2$

^aBy mixing case *a* basis functions for different electronic states one relinquishes the quantum numbers Ω , Λ , and Σ , meaning that components of angular momentum J_z , N_z , and S_z are no longer constants of the motion. Strictly speaking, \mathbf{J}^2 and J_z are the only angular momentum constants of the motion, and the more closely one approximates this mathematical requirement of angular momentum the more closely one's solutions will agree with experimental results.

diatomic Hamiltonian for a single electronic state. Table 2 gives case *a* matrix elements that mix electronic states. For a single electronic state the case *a* basis function [Eq. (19)] carries magnetic quantum numbers for more than one direction, which is ambiguous in terms of the algebraic properties of angular momentum. That is, the case *a* basis functions in Eq. (19) are not angular momentum eigenfunctions. However, a sum of such functions (in which magnetic quantum numbers for the extra component of angular momentum are mixed) does indeed satisfy the mathematical requirements for angular momentum eigenfunctions. A diatomic solution in the case *a* basis is always written as a sum for quantum numbers $\Omega = \Lambda + \Sigma$ such as ψ equal to $|^1\Sigma\rangle + |^1\Pi\rangle$, $|^2\Sigma\rangle + |^2\Pi\rangle$, $|^3\Sigma\rangle + |^3\Pi\rangle$, and $|^3\Sigma\rangle + |^3\Pi\rangle + |^1\Sigma\rangle$.

Tables 1 and 2 give the phenomenological forms of the matrix elements suitable for applied spectroscopy rather than presenting more detailed versions suitable for quantum chemistry calculations. The goal here is to develop a generic Hamiltonian subroutine that can be applied to all diatomics. In some instances accuracy is sacrificed for generality, but the loss of accuracy is typically minor. The convenience is that a single program allows us to calculate the HLFs and line positions.^{20–23} Examples are the Swan ($d^3\Pi \leftrightarrow a^3\Pi$) system of $^{12}\text{C}_2$, $^{12}\text{C}^{13}\text{C}$, $^{13}\text{C}_2$; the violet system of CN ($B^2\Sigma^+ \leftrightarrow X^2\Sigma$); and the system of CrF ($B^6\Pi \leftrightarrow X^6\Sigma^+$). The computations are sufficiently accurate in many areas of applied spectroscopy and show a standard deviation between the computed and the experimental line positions that is only two to three times larger than that obtained from a highly specialized model. To illustrate this point, Fig. 2 shows diatomic CN spectra that model measured laser-induced fluorescence spectra²⁴ and also shows computed spontaneous emission spectra.

B. HLF Algorithm

A single selection rule determines whether a term value difference represents an observable transition. That is, the transition is allowed if the HLF is nonvanishing and forbidden if the HLF is zero. To determine whether the HLF is vanishing or zero, the upper $H'(J')$ and lower $H''(J'')$ Hund's case *a*

matrix representations of Hamiltonian are diagonalized,

$$F(J') = \tilde{U}' H'(J') U', \quad (20)$$

$$F_i(J') = \sum_n \sum_m \tilde{U}_{in}' H_{nm}' U_{mi}'$$

$$= \sum_n \sum_m U_{ni} H_{nm} U_m',$$

$$F(J'') = \tilde{U}'' H(J'') U'',$$

$$F_j(J'') = \sum_n \sum_m U_{nj}'' H_{nm}'' U_{mj}'', \quad (21)$$

where U' and U'' are the orthogonal (i.e., real unitary) matrices that diagonalize $H'(J')$ and $H''(J'')$. Then the HLFs are computed,

$$S_{ij}(J', J'') = (2J'' + 1)$$

$$\times \left| \sum_n \sum_m U_{ni} \langle J'' \Omega_m'' \mathbf{q}, \Omega_n' - \Omega_m'' | J' \Omega_n' \rangle U_{mj} \right|^2, \quad (22)$$

where $\langle J'' \Omega_m'' \mathbf{q}, \Omega_n' - \Omega_m'' | J' \Omega_n' \rangle$ is the Clebsch–Gordan coefficient.

If the computed HLF $S_{ij}(J' J'')$ for the term difference $F_i(J') - F_j(J'')$ is zero (to within numerical error), the spectral line is forbidden. The concept of determining whether a term value difference represents an allowed or forbidden transition, based solely on whether the line strength for that transition is nonzero or vanishing, is not new. However, the process of finding allowed or forbidden transitions has become far easier and practical since powerful desktop computers have become commonplace.

1. Parity Algorithm

Concisely stated, the algorithm given above for computing diatomic line positions and rotational line-strength factors is (1) evaluate approximate Hamiltonians for the upper J' and lower J'' states in Hund's case *a* basis, (2) diagonalize the Hamiltonians, (3) compute vacuum wave numbers as the difference between upper and lower Hamiltonian eigenvalues, (4) compute all HLFs from the Hamilto-

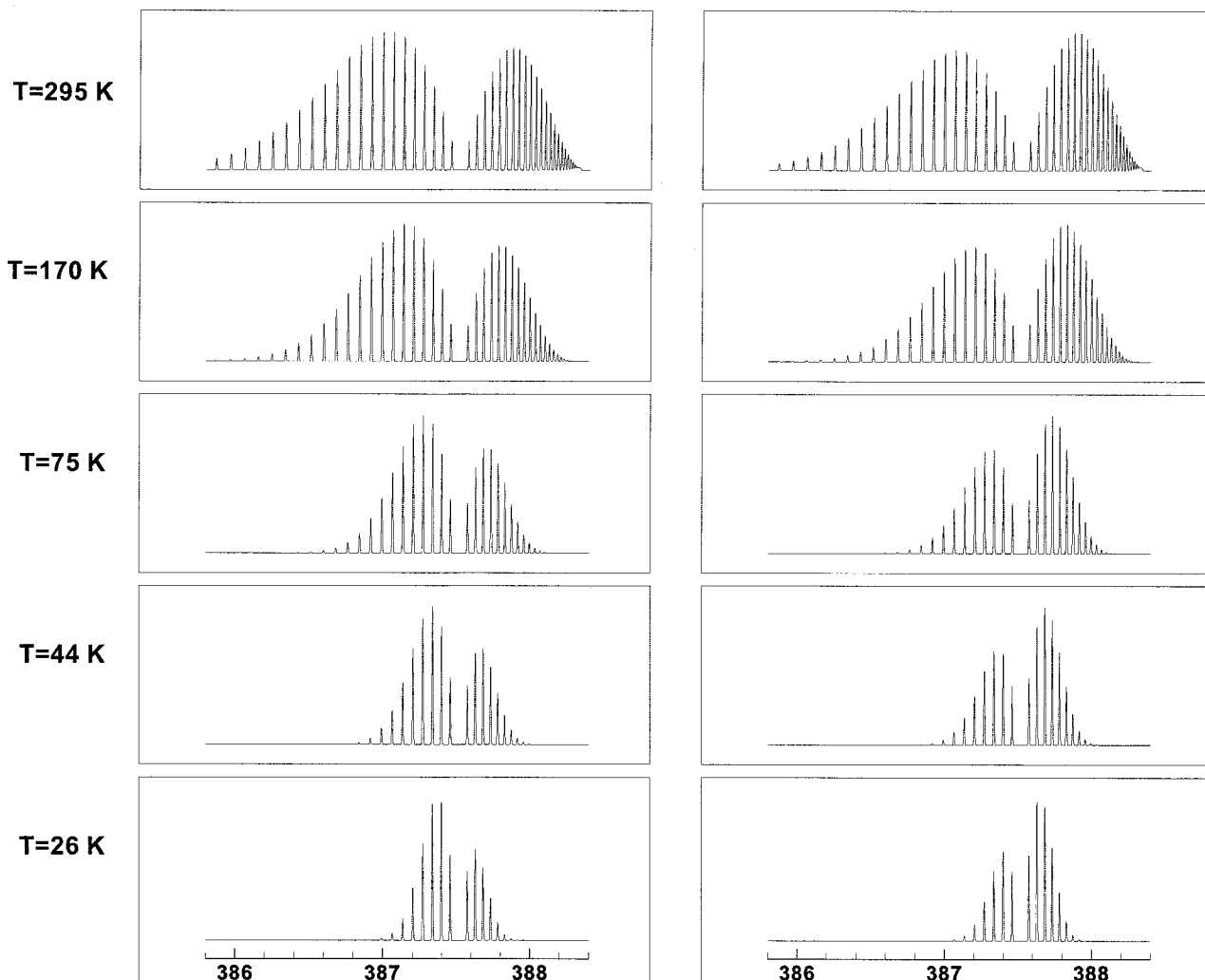


Fig. 2. Left, computed laser-induced fluorescence spectra between 386 and 388 nm of the CN radical for the indicated temperatures, to model experimental results recorded by Sims *et al.*²⁴ Right, computed free spontaneous emission spectra of the CN radical.

nian eigenvectors, and (5) discard all computed spectral lines for which the HLF vanishes. The algorithm can be applied to any member of the complete set of commuting operators (i.e., operators that can be diagonalized simultaneously, including the Hamiltonian). The parity operator commutes with the Hamiltonian if weak force terms are neglected in the Hamiltonian. Thus the algorithm for computation of the parity of diatomic states is compute the matrix representation of the Hamiltonian in the chosen basis (e.g., the Hund's case *a* basis) and subject this parity matrix to the same unitary transformation that diagonalized the Hamiltonian matrix.

The total diatomic parity can be written as the product of two factors, one of which is independent of the basis in which the parity is computed and a second basis-dependent factor. Matrix elements of the parity matrix in the Hund's case *a* basis are given by

$$p_{ij}^{(a)} = p_{\Sigma}(-)^{J+S}\delta(J_i, J_j)\delta(\Omega_i, -\Omega_j)\delta(n_i, n_j), \quad (23)$$

in which p_{Σ} is a factor independent of the basis and

the remaining terms compose the basis-dependent part. The Hund's case *b* matrix representation of parity is

$$p_{ij}^{(b)} = p_{\Sigma}(-)^{N_i}\delta(N_i, N_j)\delta(\Lambda_i, -\Lambda_j)\delta(n_i, n_j). \quad (24)$$

The parity operator P_{Σ} changes the sign on the molecule-fixed *x* component of each of the electrons. The upper $p_{\Sigma'}$ and lower $p_{\Sigma''}$ eigenvalues of this operator are fixed for a given band system. Figure 1 shows the significance of correctly assigning the values of $p_{\Sigma'}$ and lower $p_{\Sigma''}$ for a given band system.

The parity algorithm used here consists of computing the Hund's case *a* matrix representation of parity according to Eq. (23) and applying the same unitary transformation that diagonalized the Hamiltonian to the case *a* parity matrix. In the event that the case *a* Hamiltonian is nearly diagonal, its numerical diagonalization routine returns the identity matrix as the eigenvectors. The case *a* parity matrix is then diagonalized by calling the numerical diagonalization rou-

Table 3. HLFs for the Terrestrially Abundant Isotope of C_2 , $C_2(d^3\Pi_u \leftrightarrow a^3\Pi_g)$ (0,0) Band^a

J'	J''	Branch	p'	p''	N'	N''	$F_{J'}$	$F_{J''}$	$\tilde{\nu}$	$S_{J',J''}$
0.0	1.0	P_{12}	+e	-e	1	1	20928.963	1555.352	19373.611	0.96178
0.0	1.0	P_{11}	+e	-e	1	0	20928.963	1538.446	19390.517	0.03841
1.0	2.0	P_{11}	+f	-f	0	1	20916.943	1522.542	19394.401	0.06318
1.0	2.0	P_{12}	+f	-f	0	2	20916.943	1544.529	19372.414	1.45812
1.0	2.0	P_{13}	+f	-f	0	3	20916.943	1561.861	19355.082	0.00723
1.0	2.0	P_{22}	+f	-f	1	2	20932.092	1544.529	19387.564	0.03864
1.0	2.0	P_{23}	+f	-f	1	3	20932.092	1561.861	19370.232	1.93368
1.0	1.0	Q_{12}	+f	-e	0	1	20916.943	1555.352	19361.591	0.05431
1.0	1.0	Q_{11}	+f	-e	0	0	20916.943	1538.446	19378.497	1.36140
1.0	1.0	Q_{22}	+f	-e	1	1	20932.092	1555.352	19376.740	0.00325
1.0	1.0	Q_{21}	+f	-e	1	0	20932.092	1538.446	19393.647	0.08105
1.0	0.0	R_{11}	+f	-f	0	1	20916.943	1550.108	19366.834	0.05633
1.0	0.0	R_{21}	+f	-f	1	1	20932.092	1550.108	19381.984	0.94367
2.0	3.0	P_{33}	+e	-e	3	4	20941.675	1574.474	19367.201	2.93372
2.0	3.0	P_{32}	+e	-e	3	3	20941.675	1554.105	19387.570	0.02356
2.0	3.0	P_{23}	+e	-e	2	4	20923.686	1574.474	19349.212	0.00524
2.0	3.0	P_{22}	+e	-e	2	3	20923.686	1554.105	19369.581	2.60804
2.0	3.0	P_{21}	+e	-e	2	2	20923.686	1530.930	19392.756	0.04316
2.0	3.0	P_{11}	+e	-e	1	2	20902.697	1530.930	19371.767	1.71980
2.0	2.0	Q_{32}	+e	-f	3	2	20941.675	1544.529	19397.146	0.09560
2.0	2.0	Q_{33}	+e	-f	3	3	20941.675	1561.861	19379.814	0.01227
2.0	2.0	Q_{21}	+e	-f	2	1	20923.686	1522.542	19401.144	0.05588
2.0	2.0	Q_{22}	+e	-f	2	2	20923.686	1544.529	19379.157	0.71694
2.0	2.0	Q_{23}	+e	-f	2	3	20923.686	1561.861	19361.825	0.08784
2.0	2.0	Q_{11}	+e	-f	1	1	20902.697	1522.542	19380.156	3.17202
2.0	2.0	Q_{12}	+e	-f	1	2	20902.697	1544.529	19358.169	0.02739
2.0	1.0	R_{32}	+e	-e	3	1	20941.675	1555.352	19386.323	1.90991
2.0	1.0	R_{31}	+e	-e	3	0	20941.675	1538.446	19403.229	0.02524
2.0	1.0	R_{22}	+e	-e	2	1	20923.686	1555.352	19368.334	0.07075
2.0	1.0	R_{21}	+e	-e	2	0	20923.686	1538.446	19385.240	1.41308
2.0	1.0	R_{11}	+e	-e	1	0	20902.697	1538.446	19364.252	0.08082

^aAlthough one would expect to see Λ doublets in this type of band system for both *heteronuclear* and *homonuclear* molecules, half of each Λ doublet is missing here because the nuclei have zero spin-exchange symmetry prohibits one line of each Λ doublet. J' , Upper total angular momentum quantum number; J'' , Lower total angular momentum quantum number; N' , Upper total orbital angular momentum quantum number; N'' , Lower total orbital angular momentum quantum number; branch, The line designation based on J' and J'' ; p' , The upper total parity, + or -, followed by the upper e/f parity; p'' , The lower total parity, + or -, followed by the lower e/f parity; $F_{J'}$, Term computed by diagonalization of the upper Hamiltonian, cm^{-1} ; $F_{J''}$, Term computed from lower Hamiltonian, cm^{-1} ; $\tilde{\nu}$, Vacuum wavenumber computed from Hamiltonian eigenvalues, $\tilde{\nu} = F_{J'} - F_{J''}$, cm^{-1} ; $S_{J',J''}$, HLF, unitless.

tine. Once the parity is determined, the e/f parity is easily computed by standard rules.²⁵

4. Example Results from Our Program

The program output is a table of diatomic spectral line positions presented as vacuum wave numbers and the HLFs. Also output are the total parity, the e/f parity, and the branch designation (e.g., P , Q , R , . . .) Collation of all these quantities is automatic, an inherent result of the formulation. Tables 3, 4, and 5 show excerpts of the HLF table for the terrestrially abundant isotopes of C_2 , $^{12}C^{13}C$, and $^{13}C_2$. These tables were used in analyzing the Swan spectrum that occurs subsequent to laser ablation of graphite.²⁶

5. Conclusions

It is rather remarkable that the dimensions are small for a case a Hamiltonian matrix that accurately models diatomic states. However, we note

that only in the past two decades has a numerical diagonalization of thousands of mere 3×3 matrices become universally practical. Approximately a half-century passed between when the methods used in this paper were known and when their usage became practical. However, numerous ingenious analytical approximation methods were developed, many of which were milestones at the time. Unfortunately, most of these methods require a high level of expertise in molecular theory. The methods given here require some knowledge of quantum theory but not a detailed understanding of molecular theory.

The present approach shows that one merely computes the line strength for all possible term differences and discards those differences for which the strength vanishes. We emphasize that computing the strengths for all term differences and discarding those for which the strength vanishes is indeed sim-

Table 4. Diatomic HNLs for $^{12}\text{C } ^{13}\text{C}$, $^{12}\text{C } ^{13}\text{C}$ Swan ($d^3\Pi_u \leftrightarrow a^3\Pi_g$) (0,0) Band

J'	J''	Branch	p'	p''	N'	N''	$F_{J'}$	$F_{J''}$	$\tilde{\nu}$	$S_{J',J''}$
0.0	1.0	P_{12}	$-f$	$+f$	1	1	20928.877	1555.122	19373.755	0.96431
0.0	1.0	P_{11}	$-f$	$+f$	1	0	20928.877	1538.288	19390.589	0.03569
0.0	1.0	P_{11}	$+e$	$-e$	1	0	20927.642	1538.236	19389.406	0.04197
0.0	1.0	P_{12}	$+e$	$-e$	1	1	20927.642	1553.830	19373.812	0.95803
1.0	2.0	P_{11}	$-e$	$+e$	0	1	20916.771	1522.426	19394.345	0.05996
1.0	2.0	P_{12}	$-e$	$+e$	0	2	20916.771	1544.154	19372.616	1.45905
1.0	2.0	P_{13}	$-e$	$+e$	0	3	20916.771	1561.294	19355.477	0.00678
1.0	2.0	P_{23}	$+f$	$-f$	1	3	20932.965	1562.502	19370.463	1.94471
1.0	2.0	P_{22}	$+f$	$-f$	1	2	20932.965	1544.289	19388.676	0.03225
1.0	2.0	P_{13}	$+f$	$-f$	0	3	20916.831	1562.502	19354.329	0.00620
1.0	2.0	P_{12}	$+f$	$-f$	0	2	20916.831	1544.289	19372.542	1.45653
1.0	2.0	P_{11}	$+f$	$-f$	0	1	20916.831	1522.427	19394.404	0.05987
1.0	2.0	P_{22}	$-e$	$+e$	1	2	20931.791	1544.154	19387.637	0.03653
1.0	2.0	P_{23}	$-e$	$+e$	1	3	20931.791	1561.294	19370.497	1.93627
1.0	1.0	Q_{12}	$-e$	$+f$	0	1	20916.771	1555.122	19361.648	0.05079
1.0	1.0	Q_{11}	$-e$	$+f$	0	0	20916.771	1538.288	19378.483	1.37072
1.0	1.0	Q_{21}	$+f$	$-e$	1	0	20932.965	1538.236	19394.729	0.06513
1.0	1.0	Q_{11}	$+f$	$-e$	0	0	20916.831	1538.236	19378.595	1.37216
1.0	1.0	Q_{12}	$+f$	$-e$	0	1	20916.831	1553.830	19363.001	0.05984
1.0	1.0	Q_{21}	$-e$	$+f$	1	0	20931.791	1538.288	19393.503	0.07649
1.0	0.0	R_{11}	$-e$	$+e$	0	1	20916.771	1550.055	19366.716	0.05269
1.0	0.0	R_{21}	$+f$	$-f$	1	1	20932.965	1551.399	19381.567	0.95488
1.0	0.0	R_{11}	$+f$	$-f$	0	1	20916.831	1551.399	19365.433	0.04540
1.0	0.0	R_{21}	$-e$	$+e$	1	1	20931.791	1550.055	19381.736	0.94760
2.0	3.0	P_{11}	$+e$	$-e$	1	2	20902.580	1530.514	19372.066	1.71644
2.0	3.0	P_{21}	$+e$	$-e$	2	2	20923.118	1530.514	19392.605	0.04137
2.0	3.0	P_{22}	$+e$	$-e$	2	3	20923.118	1553.146	19369.972	2.61317
2.0	3.0	P_{23}	$+e$	$-e$	2	4	20923.118	1572.320	19350.798	0.00524
2.0	3.0	P_{33}	$-f$	$+f$	3	4	20941.038	1573.435	19367.603	2.93627
2.0	3.0	P_{32}	$-f$	$+f$	3	3	20941.038	1553.371	19387.668	0.02232
2.0	3.0	P_{32}	$+e$	$-e$	3	3	20939.957	1553.146	19386.811	0.02430
2.0	3.0	P_{33}	$+e$	$-e$	3	4	20939.957	1572.320	19367.637	2.92741
2.0	3.0	P_{23}	$-f$	$+f$	2	4	20923.270	1573.435	19349.834	0.00512
2.0	3.0	P_{22}	$-f$	$+f$	2	3	20923.270	1553.371	19369.899	2.60900
2.0	3.0	P_{21}	$-f$	$+f$	2	2	20923.270	1530.518	19392.751	0.04125
2.0	3.0	P_{11}	$-f$	$+f$	1	2	20902.581	1530.518	19372.063	1.71646
2.0	2.0	Q_{12}	$+e$	$-f$	1	2	20902.580	1544.289	19358.291	0.02530
2.0	2.0	Q_{11}	$+e$	$-f$	1	1	20902.580	1522.427	19380.153	3.18002
2.0	2.0	Q_{23}	$+e$	$-f$	2	3	20923.118	1562.502	19360.616	0.07105
2.0	2.0	Q_{22}	$+e$	$-f$	2	2	20923.118	1544.289	19378.829	0.72286
2.0	2.0	Q_{21}	$+e$	$-f$	2	1	20923.118	1522.427	19400.692	0.05404
2.0	2.0	Q_{32}	$-f$	$+e$	3	2	20941.038	1544.154	19396.884	0.09035
2.0	2.0	Q_{33}	$-f$	$+e$	3	3	20941.038	1561.294	19379.744	0.01082
2.0	2.0	Q_{33}	$+e$	$-f$	3	3	20939.957	1562.502	19377.455	0.01079
2.0	2.0	Q_{32}	$+e$	$-f$	3	2	20939.957	1544.289	19395.668	0.10462
2.0	2.0	Q_{21}	$-f$	$+e$	2	1	20923.270	1522.426	19400.844	0.05366
2.0	2.0	Q_{22}	$-f$	$+e$	2	2	20923.270	1544.154	19379.115	0.72408
2.0	2.0	Q_{23}	$-f$	$+e$	2	3	20923.270	1561.294	19361.976	0.08266
2.0	2.0	Q_{11}	$-f$	$+e$	1	1	20902.581	1522.426	19380.156	3.18000
2.0	2.0	Q_{12}	$-f$	$+e$	1	2	20902.581	1544.154	19358.427	0.02581
2.0	1.0	R_{11}	$+e$	$-e$	1	0	20902.580	1538.236	19364.344	0.07737
2.0	1.0	R_{21}	$+e$	$-e$	2	0	20923.118	1538.236	19384.882	1.41799
2.0	1.0	R_{22}	$+e$	$-e$	2	1	20923.118	1553.830	19369.288	0.07427
2.0	1.0	R_{32}	$-f$	$+f$	3	1	20941.038	1555.122	19385.916	1.91552
2.0	1.0	R_{31}	$-f$	$+f$	3	0	20941.038	1538.288	19402.750	0.02418
2.0	1.0	R_{31}	$+e$	$-e$	3	0	20939.957	1538.236	19401.721	0.02623
2.0	1.0	R_{32}	$+e$	$-e$	3	1	20939.957	1553.830	19386.127	1.90584
2.0	1.0	R_{22}	$-f$	$+f$	2	1	20923.270	1555.122	19368.147	0.06738
2.0	1.0	R_{21}	$-f$	$+f$	2	0	20923.270	1538.288	19384.982	1.41685
2.0	1.0	R_{11}	$-f$	$+f$	1	0	20902.581	1538.288	19364.293	0.07692

Table 5. Diatomic HNLs for $^{13}\text{C}_2$, $^{13}\text{C}_2$ Swan ($d^3\Pi_u \leftrightarrow a^3\Pi_g$) (0,0) Band

J'	J''	Branch	p'	p''	N'	N''	$F_{J'}$	$F_{J''}$	$\tilde{\nu}$	$S_{J',J''}$
0.0	1.0	P_{12}	$-f$	$+f$	1	1	20896.632	1525.302	19371.330	0.72524
0.0	1.0	P_{11}	$-f$	$+f$	1	0	20896.632	1508.563	19388.070	0.02489
0.0	1.0	P_{11}	$+e$	$-e$	1	0	20895.409	1508.514	19386.894	0.00973
0.0	1.0	P_{12}	$+e$	$-e$	1	1	20895.409	1524.002	19371.407	0.24031
1.0	2.0	P_{11}	$-e$	$+e$	0	1	20884.434	1492.711	19391.723	0.04245
1.0	2.0	P_{12}	$-e$	$+e$	0	2	20884.434	1514.208	19370.225	1.09618
1.0	2.0	P_{13}	$-e$	$+e$	0	3	20884.434	1531.123	19353.311	0.00501
1.0	2.0	P_{23}	$+f$	$-f$	1	3	20900.527	1532.345	19368.182	0.48716
1.0	2.0	P_{22}	$+f$	$-f$	1	2	20900.527	1514.335	19386.191	0.00765
1.0	2.0	P_{12}	$+f$	$-f$	0	2	20884.489	1514.335	19370.154	0.36469
1.0	2.0	P_{11}	$+f$	$-f$	0	1	20884.489	1492.712	19391.778	0.01410
1.0	2.0	P_{22}	$-e$	$+e$	1	2	20899.359	1514.208	19385.150	0.02597
1.0	2.0	P_{23}	$-e$	$+e$	1	3	20899.359	1531.123	19368.236	1.45599
1.0	1.0	Q_{12}	$-e$	$+f$	0	1	20884.434	1525.302	19359.131	0.03546
1.0	1.0	Q_{11}	$-e$	$+f$	0	0	20884.434	1508.563	19375.871	1.03450
1.0	1.0	Q_{21}	$+f$	$-e$	1	0	20900.527	1508.514	19392.013	0.01519
1.0	1.0	Q_{11}	$+f$	$-e$	0	0	20884.489	1508.514	19375.975	0.34531
1.0	1.0	Q_{12}	$+f$	$-e$	0	1	20884.489	1524.002	19360.487	0.01401
1.0	1.0	Q_{21}	$-e$	$+f$	1	0	20899.359	1508.563	19390.796	0.05321
1.0	0.0	R_{11}	$-e$	$+e$	0	1	20884.434	1520.403	19364.030	0.03678
1.0	0.0	R_{21}	$+f$	$-f$	1	1	20900.527	1521.752	19378.775	0.23947
1.0	0.0	R_{11}	$+f$	$-f$	0	1	20884.489	1521.752	19362.737	0.01053
1.0	0.0	R_{21}	$-e$	$+e$	1	1	20899.359	1520.403	19378.956	0.71322
2.0	3.0	P_{11}	$+e$	$-e$	1	2	20870.198	1500.512	19369.685	0.42868
2.0	3.0	P_{21}	$+e$	$-e$	2	2	20890.541	1500.512	19390.029	0.00992
2.0	3.0	P_{22}	$+e$	$-e$	2	3	20890.541	1522.849	19367.692	0.65427
2.0	3.0	P_{33}	$-f$	$+f$	3	4	20908.228	1542.791	19365.437	2.20554
2.0	3.0	P_{32}	$-f$	$+f$	3	3	20908.228	1523.063	19385.165	0.01630
2.0	3.0	P_{32}	$+e$	$-e$	3	3	20907.146	1522.849	19384.297	0.00590
2.0	3.0	P_{33}	$+e$	$-e$	3	4	20907.146	1541.657	19365.489	0.73356
2.0	3.0	P_{22}	$-f$	$+f$	2	3	20890.682	1523.063	19367.619	1.95922
2.0	3.0	P_{21}	$-f$	$+f$	2	2	20890.682	1500.517	19390.165	0.02947
2.0	3.0	P_{11}	$-f$	$+f$	1	2	20870.199	1500.517	19369.682	1.28580
2.0	2.0	Q_{12}	$+e$	$-f$	1	2	20870.198	1514.335	19355.862	0.00600
2.0	2.0	Q_{11}	$+e$	$-f$	1	1	20870.198	1492.712	19377.486	0.79708
2.0	2.0	Q_{23}	$+e$	$-f$	2	3	20890.541	1532.345	19358.196	0.01672
2.0	2.0	Q_{22}	$+e$	$-f$	2	2	20890.541	1514.335	19376.206	0.18230
2.0	2.0	Q_{21}	$+e$	$-f$	2	1	20890.541	1492.712	19397.829	0.01272
2.0	2.0	Q_{32}	$-f$	$+e$	3	2	20908.228	1514.208	19394.019	0.06407
2.0	2.0	Q_{33}	$-f$	$+e$	3	3	20908.228	1531.123	19377.105	0.00717
2.0	2.0	Q_{32}	$+e$	$-f$	3	2	20907.146	1514.335	19392.811	0.02456
2.0	2.0	Q_{21}	$-f$	$+e$	2	1	20890.682	1492.711	19397.971	0.03774
2.0	2.0	Q_{22}	$-f$	$+e$	2	2	20890.682	1514.208	19376.473	0.54827
2.0	2.0	Q_{23}	$-f$	$+e$	2	3	20890.682	1531.123	19359.559	0.05889
2.0	2.0	Q_{11}	$-f$	$+e$	1	1	20870.199	1492.711	19377.488	2.39150
2.0	2.0	Q_{12}	$-f$	$+e$	1	2	20870.199	1514.208	19355.991	0.01825
2.0	1.0	R_{11}	$+e$	$-e$	1	0	20870.198	1508.514	19361.683	0.01823
2.0	1.0	R_{21}	$+e$	$-e$	2	0	20890.541	1508.514	19382.027	0.35533
2.0	1.0	R_{22}	$+e$	$-e$	2	1	20890.541	1524.002	19366.539	0.01760
2.0	1.0	R_{32}	$-f$	$+f$	3	1	20908.228	1525.302	19382.926	1.43987
2.0	1.0	R_{31}	$-f$	$+f$	3	0	20908.228	1508.563	19399.665	0.01730
2.0	1.0	R_{31}	$+e$	$-e$	3	0	20907.146	1508.514	19398.632	0.00622
2.0	1.0	R_{32}	$+e$	$-e$	3	1	20907.146	1524.002	19383.145	0.47745
2.0	1.0	R_{22}	$-f$	$+f$	2	1	20890.682	1525.302	19365.380	0.04759
2.0	1.0	R_{21}	$-f$	$+f$	2	0	20890.682	1508.563	19382.119	1.06565
2.0	1.0	R_{11}	$-f$	$+f$	1	0	20870.199	1508.563	19361.636	0.05446

ple to implement in a computer program, and the implementation is computationally fast.

References

1. Von H. Hönl and F. London, "Über die Intensitäten der Bandenlinien," *Z. Phys.* **33**, 803–809 (1925).
2. F. Roux, M. Michaud, and M. Vervloet, "High-resolution Fourier spectrometry of $^{14}\text{N}_2$: analysis of the (0-0), (0-1), (0-2), (0-3) bands of the $C^3\Pi_u \leftrightarrow B^3\Pi_g$ system," *Can. J. Phys.* **67**, 143–147 (1989).
3. A. P. Thorne, *Spectrophysics* (Chapman & Hall, 1974, 1988).
4. A. P. Thorne, U. Litzen, and S. Johansson, *Spectrophysics: Principles and Applications* (Springer-Verlag, 1999).
5. R. C. Hilborn, "Einstein coefficients, cross sections, f values, dipole moments, and all that," *Am. J. Phys.* **50**, 982–986 (1982).
6. E. U. Condon and G. H. Shortly, *The Theory of Atomic Spectra* (Cambridge U. Press, 1964).
7. I. I. Sobelman, *Atomic Spectra and Radiative Transitions* (Springer-Verlag, 1979).
8. H. Lefebvre-Brion and R. W. Field, *Perturbations in the Spectra of Diatomic Molecules* (Academic, 1986).
9. H. Lefebvre-Brion and R. W. Field, *The Spectra and Dynamics of Diatomic Molecules* (Elsevier, 2004).
10. P. L. Rubin, "Line intensity factors in electronic spectra of diatomic molecules," *Opt. Spectrosc.* **20**, 325–327 (1966).
11. I. Kovacs, *Rotational Structure in the Spectra of Diatomic Molecules*, L. Nemes, transl. (American Elsevier, 1969).
12. J. T. Hougen, *The Calculation of Rotational Energy Levels and Rotational Line Intensities in Diatomic Molecules*, version 1.0, NBS Monograph 115 (National Institute of Standards and Technology, 1970), <http://physics.nist.gov/DiatomCalculations> [2004, February 2].
13. A. Schadee, "The relation between the electronic oscillator strength and the wavelength of diatomic molecules," *J. Quant. Spectrosc. Radiat. Transfer* **7**, 169–183 (1967).
14. A. Schadee, "On the normalization of Hönl–London factors," *Astron. Astrophys.* **14**, 401–404 (1971).
15. A. Schadee, "Theory of first rotational lines in transitions of diatomic molecules," *Astron. Astrophys.* **41**, 203–212 (1975).
16. J. B. Tatum, "The interpretation of intensities in diatomic molecular spectra," *Astrophys. J. Suppl.* **14**, 21–55 (1967), 22, 388 (1971).
17. E. E. Whiting, J. A. Paterson, I. Kovacs, and R. W. Nicholls, "Computer checking of rotational line intensity factors for diatomic molecules," *J. Mol. Spectrosc.* **47**, 84–98 (1973).
18. E. E. Whiting and R. W. Nicholls, "Reinvestigation of rotational line strength factors in diatomic spectra," *Astrophys. J. Suppl.* **27**, 1–19 (1974).
19. J. O. Hornkohl and C. Parigger, "Angular momentum states of the diatomic molecule," *Am. J. Phys.* **64**, 623–632 (1996).
20. J. O. Hornkohl and C. G. Parigger, "Boltzmann equilibrium spectrum program (BESP)," <http://view.utsi.edu/besp>.
21. J. O. Hornkohl, C. Parigger, and J. W. L. Lewis, "Temperature-measurements from CN spectra in a laser-induced plasma," *J. Quant. Spectrosc. Radiat. Transfer* **46**, 405–411 (1991).
22. C. Parigger, D. H. Plemmons, J. O. Hornkohl, and J. W. L. Lewis, "Spectroscopic temperature measurements in a decaying laser-induced plasma using the C_2 Swan system," *J. Quant. Spectrosc. Radiat. Transfer* **52**, 707–711 (1994).
23. C. G. Parigger, G. Guan, and J. O. Hornkohl, "Measurement and analysis of OH emission spectra following laser-induced breakdown," *Appl. Opt.* **30**, 5986–5991 (2003).
24. I. R. Sims, J.-L. Queffelec, A. Defrance, C. Rebrion-Rowe, D. Travers, P. Bocherel, and I. W. M. Smith, "Ultralow temperature kinetics of neutral–neutral reactions. The technique and results for the reactions $\text{CN} + \text{O}_2$ down to 13 K and $\text{CN} + \text{NH}$ down to 25 K," *J. Chem. Phys.* **100**, 4229–4241 (1994).
25. J. M. Brown, J. T. Hougen, K. P. Huber, J. W. C. Johns, I. Kopp, H. Lefebvre-Brion, A. J. Merer, D. A. Ramsay, J. Rostas, and R. N. Zare, "The labeling of parity doublet levels in linear molecules," *J. Mol. Spectrosc.* **55**, 500–503 (1975).
26. C. G. Parigger, J. O. Hornkohl, A. M. Keszler, and L. Nemes, "Measurement and analysis of atomic and diatomic carbon spectra from laser ablation of graphite," *Appl. Opt.* **30**, 6192–6198 (2003).